



THE PENNSYLVANIA
STATE UNIVERSITY

IONOSPHERIC RESEARCH

Scientific Report 393

THE PHOTOLYSIS OF CH₃ONO

by

H. A. Wiebe and Julian Heicklen

June 23, 1972

*This research in this document has been sponsored by the
National Aeronautics and Space Administration under Grant No.
NRL 39-009-003.*

Reproduced by
NATIONAL TECHNICAL
INFORMATION SERVICE
US Department of Commerce
Springfield, VA. 22151

IONOSPHERE RESEARCH LABORATORY

(NASA-CR-131355) THE PHOTOLYSIS OF
CH₃ONO (Pennsylvania State Univ.)
HC ~~XXXXXXXXXX~~

33 p
CSCL 04A

N73-20425

Unclas

G3/13 17402

University Park, Pennsylvania

PSU-IRL-SCI 393

Scientific Report 393

"The Photolysis of CH_3ONO "

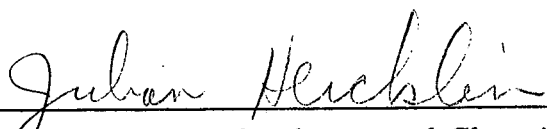
by

H. A. Wiebe and Julian Heicklen

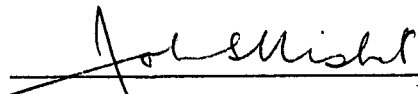
June 23, 1972

"The research in this document has been sponsored by the National Aeronautics and Space Administration under Grant No. NHL 39-009-003."

Submitted by:

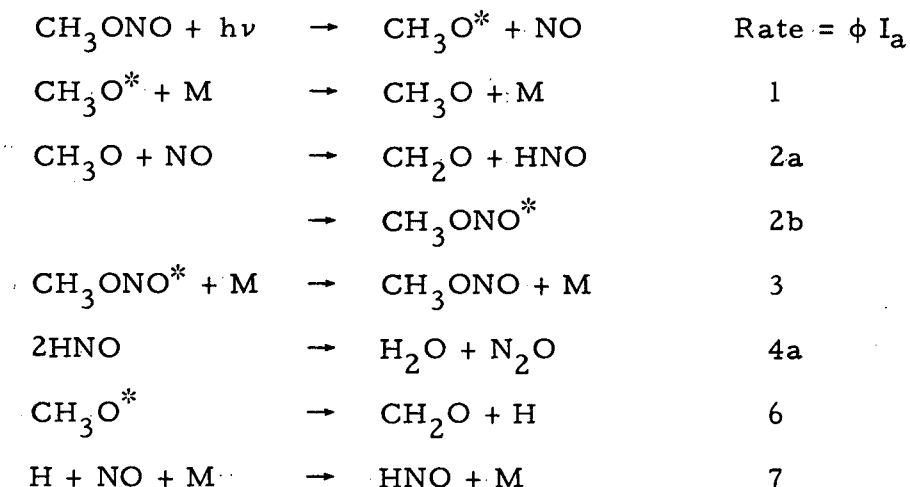

Julian Heicklen, Professor of Chemistry
Project Supervisor

Approved by:

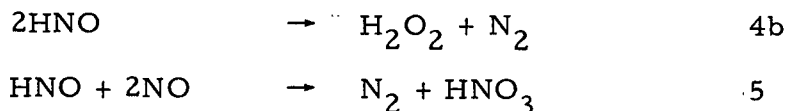

John S. Nisbet, Director
Ionosphere Research Laboratory

Ionosphere Research Laboratory
The Pennsylvania State University
University Park, Pennsylvania 16802

The photolysis of CH_3ONO , alone and in the presence of NO , $\text{NO}-\text{N}_2$ mixtures, and $\text{NO}-\text{CO}$ mixtures was studied between 25 and 150°C. The major products are CH_2O , N_2O , and H_2O . We have not measured CH_2O and H_2O , but have measured the quantum yields of N_2O . The steps responsible for these products are

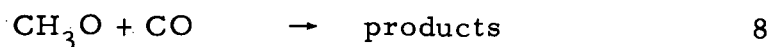


The N_2O yield is large at low pressures but approaches a high-pressure limiting value of 0.055 at all temperatures as the excited CH_3O (CH_3O^*) produced in the primary step is stabilized by collision. With this value and the primary quantum yield of 0.76 for reaction 1, the ratio $k_{2a}/k_2 = 0.145$ where $k_2 \equiv k_{2a} + k_{2b}$. Nitrogen is also a product of the reaction and is produced from two sources



where $k_{4a}/k_{4b} = 51$ at all temperatures. Reaction 5 is second-order in $[\text{NO}]$ at low $[\text{NO}]$, but becomes first-order in $[\text{NO}]$ at high $[\text{NO}]$.

In the presence of excess CO , the N_2O yield drops, and CO_2 is produced (though not in sufficient amounts to account for the drop in N_2O). The indicated additional reaction is



with $k_8/k_2 \sim 5 \times 10^{-4}$ at all temperatures.

When pure CH_3ONO is photolyzed, CO is produced and NO accumulates in the system. Both products are formed in related processes and result from

CH₃O attack on CH₂O

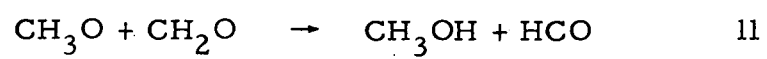


TABLE OF CONTENTS

	Page
ABSTRACT	i
INTRODUCTION	1
EXPERIMENTAL	3
Materials	3
Apparatus and Analysis	3
Actinometry	4
RESULTS	5
DISCUSSION	7
ACKNOWLEDGEMENTS	13
REFERENCES	14
LIST OF FIGURES	21

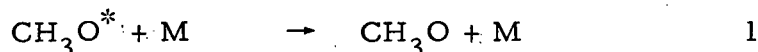
Introduction

The methoxy radical is present in both the upper and lower atmospheres. In the upper atmosphere it is produced from the oxidation of CH_3 , which in turn comes from either the photolysis of CH_4 or the reactions of CH_4 with $\text{O}(^1\text{D})$ or HO . In the lower atmosphere CH_3O is an intermediate in the photochemical oxidation of hydrocarbons, and it may be important in the conversion of NO to NO_2 in polluted urban atmospheres.¹

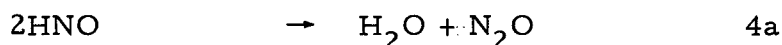
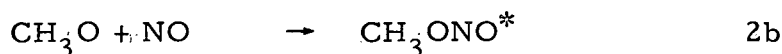
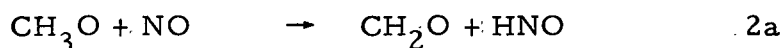
Because of the importance of CH_3O in the atmosphere, we have initiated studies of the reactions of this radical with other atmospheric gases such as NO , CO , O_2 , NO_2 , and SO_2 . As a source of CH_3O , the photolysis of CH_3ONO was used. A number of previous investigators²⁻¹⁰ have shown that CH_3ONO photodecomposes readily via



though the primary quantum yield might be less than unity.⁹ Other studies in our laboratory have now established that ϕ , the primary quantum yield, is 0.76.¹¹ The asterisk on CH_3O indicates that it may contain excess energy and require deactivation to be stabilized.



As the reaction proceeds, the major products are CH_2O , N_2O and H_2O . These products can be attributed to the reactions of CH_3O with NO



The presence of HNO has been definitely established,^{3,9} and Napier and Norrish, as well as other studies in our laboratory,¹¹ have shown that it arises principally (if not entirely) from reaction 2a and not from the primary photolytic act. Furthermore, McGraw and Johnston¹⁰ found $\phi k_{2a}/k_2 = 0.11$ at room temperature, where $k_2 = k_{2a} + k_{2b}$. They reasonably, but erroneously, assumed that $\phi = 1.0$ and thus deduced that $k_{2b}/k_{2a} = 8.0$.

This system appeared to be well characterized. However, as our work progressed, other previously unreported effects were apparent. Thus we have re-examined the photolysis of CH_3ONO and $\text{CH}_3\text{ONO-NO}$ mixtures at 3660Å in detail. In the latter case, experiments were also done with excess N_2 or CO present. The results of these studies are reported here.

Experimental

Materials: Methyl nitrite was prepared by the dropwise addition of 30% H_2SO_4 to a saturated solution of NaNO_2 in methyl alcohol. An oxygen-free N_2 stream was used to carry the gaseous methyl nitrite through traps of ascarite, potassium bicarbonate and mercury before being condensed at -80°C . The pale yellow product was then fractionated in vacuo (-110° to -130°) and stored in a darkened flask at -196° .

Azomethane was prepared from dimethyl hydrazine and mercuric oxide by Renaud and Leitch's method.¹² It was purified by distillation under vacuum (-110° to -130°) and stored at -196° .

C.P. grade N_2 and CO from the Matheson Co. were purified by slow passage through a trap filled with glass wool at liquid argon temperature, resulting in the complete removal of the CO_2 impurity. Nitric oxide (Matheson Co.) was fractionally distilled under vacuum to remove all impurities.

Apparatus and Analysis: The photolysis took place in a cylindrical (50 x 100 mm) quartz reaction cell enclosed in an aluminum block furnace. Temperature regulation within 0.1° was achieved by a bridge circuit temperature control (Cole-Parmer Inst. Co.). A conventional vacuum line, kept grease-free through the use of Teflon stopcocks with Viton "O" rings, was used to store and transfer the reagents to the reaction cell. The radiation sources were Hanovia, type 30620, medium pressure mercury arcs, and were used in conjunction with 0-52 and 7-54 Corning glass filters to isolate the 3660\AA line.

All products were analyzed by gas chromatography using a thermistor detector. A 3-meter, type Q-S Porapak column, at 0° and He flow rate of 60 cc/min was used to measure the N_2O and CO_2 . In experiments with added CO and N_2 , the excess reactants were removed by slow passage through two traps filled with glass wool at -196° . The non-condensable gases, NO , N_2 , and CO , were collected with a Toepler pump and analyzed on a 2-meter 5\AA Molecular Sieve Column at 40° and a He flow rate of 50 cc/min.

Actinometry: Quantum yields were based on light intensities measured by the photolysis of azomethane. The non-condensable gases, N_2 and CH_4 , were collected with a Toepler pump and analyzed by gas chromatography on the 5 \AA Molecular Sieve Column. For the conditions of the experiments $\Phi\{N_2\} = 1.13$

Absorption of the 3660 \AA radiation by reagent and actinometer gases was matched at all temperatures. Extinction coefficients were determined by using the lamp-filter combination as a light source and an RCA 935 phototube to measure the radiation. For methyl nitrite and azomethane the extinction coefficient (to base 10) were: 2.48×10^{-3} , 2.18×10^{-3} , 1.91×10^{-3} and $1.76 \times 10^{-3} \text{ Torr}^{-1} \text{ cm}^{-1}$ for methyl nitrite and 1.87×10^{-4} , 1.73×10^{-4} , 1.64×10^{-4} and $1.59 \times 10^{-4} \text{ Torr}^{-1} \text{ cm}^{-1}$ for azomethane at 25 $^\circ$, 80 $^\circ$, 125 $^\circ$, and 150 $^\circ$ respectively.

Results

Mixtures of CH_3ONO and NO were photolyzed at 25, 80, and 150°C . The products measured were N_2O and N_2 . No attempt was made to analyze for either CH_2O or H_2O . At 150°C , some pyrolysis of CH_3ONO also was observed in conformance with the findings of Phillips.¹⁴ However, the pyrolytic reaction was much less important than the photolytic reaction, and all the reported quantum yields have been corrected for the pyrolytic reaction as measured in separate dark runs.

Initially, mixtures of 30 Torr CH_3ONO and about 1 Torr of NO were photolyzed to various extents of conversions at the three temperatures. The quantum yield of N_2O , $\Phi\{\text{N}_2\text{O}\}$, was monitored and the results are shown in Table I. For these pressures $\Phi\{\text{N}_2\text{O}\}$ was about 0.075 independent of the extent of conversion and nearly independent of the temperature.

Next, a series of runs was done at 25°C for various mixtures of NO and CH_3ONO . The results are shown in Table II. For $[\text{NO}] \sim 1$ Torr, the N_2 is almost undetectable. $\Phi\{\text{N}_2\text{O}\}$ drops from 0.25 at $[\text{CH}_3\text{ONO}] = 2.3$ Torr to about 0.055 for high CH_3ONO pressures. However, as $[\text{NO}]$ is augmented, $\Phi\{\text{N}_2\}$ increases in importance, and this increase is accompanied by a decrease in $\Phi\{\text{N}_2\text{O}\}$ until ultimately $\Phi\{\text{N}_2\} > \Phi\{\text{N}_2\text{O}\}$.

In order to see if the drop in $\Phi\{\text{N}_2\text{O}\}$ with increasing $[\text{CH}_3\text{ONO}]$ was due to chemical reaction or an inert gas effect, experiments were done with excess N_2 added. These results are shown in Table III. The addition of N_2 reduced $\Phi\{\text{N}_2\text{O}\}$ at all three temperatures, and the same limiting value of about 0.055 was obtained.

Experiments with excess CO added are shown in Table IV. Calvert¹⁵ had evidence that CH_3O could react with CO to produce CO_2 , and we wished to verify this observation. We do find that CO_2 is produced, though in small amounts, but its quantum yield increases with $[\text{CO}]/[\text{NO}]$. Furthermore, at the higher temperatures, $\Phi\{\text{N}_2\text{O}\}$ is reduced below the value found at high pressures of CH_3ONO or N_2 in the absence of CO . This additional reduction in $\Phi\{\text{N}_2\text{O}\}$ is further evidence that

CO is removing CH_3O radicals, thus diminishing the importance of reaction 2a.

Finally, three series of runs were done with pure CH_3ONO at the same molar concentration and with the same absorbed intensity, I_a , but at 25, 80, and 125°C . The last series was done at 125° rather than 150°C to eliminate the dark reaction. In each series, runs were done for different irradiation times, and four of the products (N_2O , N_2 , CO, and NO) were monitored. Methanol was also found, but quantitative analysis was not done. The results are shown in Figs. 1-4.

The amounts of N_2O and N_2 as a function of irradiation time are shown in Figs. 1 and 2, respectively. Both products show an induction period of about 4 minutes, but then grow linearly with time, the rate of growth being independent of temperature. The quantum yields obtained from the slope of the straight line portion, $\Phi_f\{\text{N}_2\text{O}\}$ and $\Phi_f\{\text{N}_2\}$, are listed in Table V. $\Phi_f\{\text{N}_2\text{O}\}$ is similar to $\Phi\{\text{N}_2\text{O}\}$ for runs with about 1 Torr of NO initially added at the same CH_3ONO pressure.

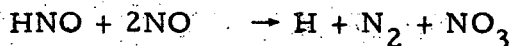
Fig. 3 shows the amount of CO produced vs. irradiation time. There is a significant induction period (15-35 min.), after which CO grows linearly with time. The quantum yields obtained from the linear portions, $\Phi_f\{\text{CO}\}$, increase with temperature and they are listed in Table V. The amount of NO produced vs. irradiation time is shown in Fig. 4. The NO rises rapidly for about 20 min., after which it grows linearly at a slower rate. The quantum yields obtained from the slope of the later linear period, $\Phi_f\{\text{NO}\}$, also increase with temperature and they are listed in Table V.

The results of the photolysis of $\text{CH}_3\text{ONO-NO}$ mixtures are generally consistent with the mechanism consisting of the reactions listed in the Introduction. However, there are two observations not explained by the mechanism. These are the production of N_2 and the pressure dependence of $\Phi\{\text{N}_2\text{O}\}$.

The production of N_2 at high NO pressures can be attributed to the reaction of NO with HNO. This reaction has been reported previously, but two different mechanisms have been suggested.¹⁶



or



followed by

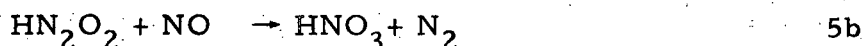


In the former case, since HNO is consumed, the N_2 should be formed at the expense of N_2O . In the latter case, HNO is regenerated and $\Phi\{\text{N}_2\text{O}\}$ should be unaffected. The results in Table II clearly support the former case, reaction 5. In fact, if reaction 5 is operable, then $2\Phi\{\text{N}_2\text{O}\} + \Phi\{\text{N}_2\}$ should be constant at any pressure of CH_3ONO . This sum is listed in Table II and the expectation is confirmed.

Reaction 5 is an overall reaction which is presumably first-order in $[\text{HNO}]$, but of unknown order in $[\text{NO}]$. The mechanism predicts that

$$I_a^{1/2} \Phi\{\text{N}_2\} / (\Phi\{\text{N}_2\text{O}\})^{1/2} = k_5 [\text{NO}]^n / k_{4a}^{1/2} \quad I$$

where n is the order of reaction 5 with respect to $[\text{NO}]$. Fig. 5 is a log-log plot of the left-hand side of eqn. I vs. $[\text{NO}]$. The plot is not linear, but at low $[\text{NO}]$ approaches a slope of two; and at high $[\text{NO}]$, approaches a slope of about one. Thus, reaction 5 itself is a complex reaction which can be represented by¹⁶



The expanded rate law then becomes

$$I_a^{1/2} \Phi \{N_2\} / \Phi \{N_2O\}^{1/2} = k_{5a} k_{5b} [NO]^2 / k_{4a}^{1/2} (k_{-5a} + k_{5b} [NO]) \quad II$$

At low $[NO]$, $n = 2$, and $k_5 = k_{5a} k_{5b} / k_{-5a}$; while at high $[NO]$, $n = 1$, and $k_5 = k_{5a}$. Values for the appropriate ratios are listed in Table VI.

The other unexpected result is the pressure dependence of $\Phi \{N_2O\}$, which can be attributed to an inert gas effect, since N_2 also produces the effect. There are three possible explanations: 1) Energetic CH_3O radicals are formed in the primary process which have a value different than thermal CH_3O for k_{2a}/k_{2b} , 2) The energetic CH_3ONO^* produced in reaction 2b can redissociate unless stabilized by collision, or 3) Energetic CH_3O radicals formed in the primary process can dissociate before collisional stabilization.



The H atoms would be scavenged by NO to produce HNO



In the first case, $2\Phi \{N_2O\} + \Phi \{N_2\}$ should depend on the ratio $[M]/[NO]$, whereas in cases 2 and 3, $2\Phi \{N_2O\} + \Phi \{N_2\}$ should depend only on $[M]$, where $[M]$ is the total effective concentration of quenching gas. The results in Table II show no inverse dependence on $[NO]$ and thus the first possibility is eliminated.

The second possibility cannot be ruled out on the basis of the information here, but can be shown to be unlikely from a consideration of the thermal decomposition of CH_3ONO , which was studied long ago by Steacie and Shaw.¹⁷ They found the decomposition to be first-order even at 33 torr at 230°C. Since at lower temperatures, the first-order regime should extend to even lower pressures, it is unlikely that reaction -2b could compete with reaction 3 under our experimental conditions.

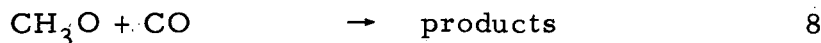
The most likely explanation for the pressure dependence is the third of the above possibilities. There is evidence for "hot" radical production in the photolysis of the higher alkyl nitrites,^{18, 19} though not in C_2H_5ONO at 3660 Å.²⁰

With reactions 5-7 included, the mechanism predicts that

$$2 \Phi \{N_2O\} + \Phi \{N_2\} = \frac{(k_6 + k_1 k_{2a} [M] / k_2) \phi}{k_1 [M] + k_6} \quad \text{III}$$

where $k_2 = k_{2a} + k_{2b}$. Fig. 6 is a plot of $2\Phi\{N_2O\} + \Phi\{N_2\}$ vs. $[CH_3ONO]^{-1}$ at $25^\circ C$ for runs in which CH_3ONO is the principal deactivating gas. The intercept gives $\phi k_{2a} / k_2 = 0.11$. Earlier results¹⁶ suggested a value of 0 at $25^\circ C$. However, our value agrees exactly with that of McGraw and Johnston,¹⁰ who photolyzed 1 Torr of CH_3ONO in the presence of 1 atm of N_2 . Consequently, their observed branching ratio is for the high-pressure limiting case. Our results in Tables I and III and Fig 1 indicate that this ratio is independent of temperature. The only other high-temperature value reported for k_{2a}/k_2 is 0.33 at $174^\circ C$.²¹ Unfortunately, the reactant pressures are not given, but presumably they were below those necessary to completely stabilize CH_3O^* and the reported branching ratio is greater than k_{2a}/k_2 . The slope of the linear portion of Fig. 6 gives $k_6/k_1 = 1.94$ Torr for CH_3ONO as the quenching gas. As $[CH_3ONO]^{-1}$ becomes very large, the ordinate of Fig. 6 should approach ϕ . It is clear from the graph that this value is significantly less than unity and greater than 0.5. The limiting value was not achieved under the experimental conditions used here, but the value of 0.76 was found elsewhere.¹¹

For reaction mixtures with excess CO added, an additional reaction must be added.



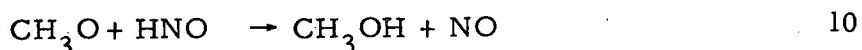
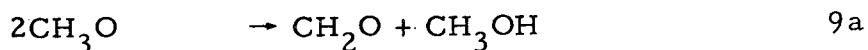
If every time reaction 8 occurred CO_2 was produced, then the drop in $\Phi\{N_2O\}$ should be $0.055 \Phi\{CO_2\}$ and

$$\Phi\{CO_2\} / \Phi\{N_2O\} = 2k_8 [CO] / k_{2a} [NO] \quad \text{IV}$$

Fig. 7 is a log-log plot of $\Phi\{CO_2\} / \Phi\{N_2O\}$ vs. $[CO]/[NO]$ at $150^\circ C$. A reasonable straight line of unit slope can be drawn through the points which yield a value of 2.4×10^{-4} for k_8/k_{2a} . However, the data in Table IV indicate

that the fall-off in $\Phi\{\text{N}_2\text{O}\}$ is very much greater than $0.055 \Phi\{\text{CO}_2\}$, so that k_8/k_{2a} may be about 10 times larger. This discrepancy between the fall-off in $\Phi\{\text{N}_2\text{O}\}$ and $0.055 \Phi\{\text{CO}_2\}$ is much more pronounced at the lower temperatures. Also, at the lower temperatures $\Phi\{\text{CO}_2\}$ increases much slower than first-order in $[\text{CO}]/[\text{NO}]$. Apparently the principal product is not CO_2 , but perhaps $(\text{CH}_3\text{O})_2\text{CO}$ or $(\text{CH}_3\text{OCO})_2$. From the fall-off in $\Phi\{\text{N}_2\text{O}\}$, k_8/k_2 is estimated to be $\sim 5 \times 10^{-4}$ at 80 and 150°C. An estimate at room temperature is difficult to make because so little CO_2 was produced that it was necessary to work at low NO pressures. A very rough estimate would be about 10^{-4} but this is probably low because significant amounts of NO are being produced during the run. In all likelihood, $k_8/k_2 \sim 5 \times 10^{-4}$ almost independent of temperature. Furthermore, most of the time that reaction 6 proceeds, CO_2 is not produced.

If pure CH_3ONO is photolyzed, then NO , which is not present initially, accumulates in the system. In the early stages, the CH_3O radicals are removed via



However, very quickly the NO pressure becomes sufficient to suppress these reactions, reactions 2a and 2b dominate, and N_2O is produced. This is shown in Fig. 1 where N_2O grows linearly with time after a short induction period of about 4 minutes. At 4 minutes $[\text{NO}] \sim 5 \times 10^{-6} \text{M}$, as seen from Fig. 4. The rate of reaction 9, $R\{9\}$, relative to that for reaction 2, $R\{2\}$, is given by

$$R\{9\}/R\{2\} = k_9 I_a / k_2^2 [\text{NO}]^2 \quad \text{V}$$

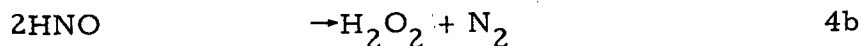
Since k_9 has been estimated²² to be $10^{9.9} \text{M}^{-1} \text{sec}^{-1}$ and k_2 has been estimated²¹ to be $5 \times 10^7 \text{M}^{-1} \text{sec}^{-1}$, reaction 9 can be shown to be only one per cent as important as reaction 2 at this pressure of NO , and it decreases in importance as $[\text{NO}]^2$.

The relative importance of reaction 10 can be estimated from

$$R\{10\}/R\{2\} = k_{10} (\Phi_f \{ \text{N}_2\text{O} \} I_a / k_{4a})^{1/2} / k_2 [\text{NO}] \quad \text{VI}$$

At the end of the induction period, where $[\text{NO}] \sim 5 \times 10^{-6} \text{M}$, $R\{10\} \sim R\{2\}$. The rate constant k_{10} has been estimated¹⁰ to be $3 \times 10^{10} \text{M}^{-1} \text{sec}^{-1}$. Thus k_{4a} must be about $10^8 \text{M}^{-1} \text{sec}^{-1}$ which is about 100 times larger than that for DNO .¹⁶

The rate of growth of N_2 (Fig. 2) exactly parallels that for N_2O and is independent of $[\text{NO}]$. The indicated reaction is

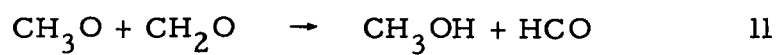


where the reaction probably involves the isomeric HON form of HNO and proceeds through a four-center intermediate. The ratio k_{4a}/k_{4b} is given by $\Phi_f \{ \text{N}_2\text{O} \} / \Phi_f \{ \text{N}_2 \}$ and is 51.

It is still necessary to explain both the CO and NO production after the induction period. Figs. 3 and 4 show that these products grow linearly with time after the

induction period, the rate of production of each increasing with temperature.

CO production must come from CH_2O removal and NO production from CH_3O removal. The indicated reaction is



The HCO radical must be scavenged by NO to ultimately produce CO.^{8, 23}

Acknowledgement

The authors wish to thank Dr. Alberto Villa for helpful advice. This work was supported by the National Aeronautics and Space Administration under Grant No. NGL 39-009-003 for which we are grateful.

References

1. J. Heicklen, K. Westberg, and N. Cohen, "The Conversion of NO to NO₂ in Polluted Atmospheres," The Pennsylvania State University, Center for ²Air Environment Studies, Publication No. 115-69 (1969).
2. J. A. Gray and D. W. G. Style, Trans. Faraday Soc., 48, 1137 (1952).
3. H. W. Brown and G. C. Pimentel, J. Chem. Phys., 29, 883 (1958).
4. P. L. Hanst and J. G. Calvert, J. Phys. Chem., 63, 2071 (1959).
5. B. H. J. Bielski and R. B. Timmons, J. Phys. Chem., 68, 347 (1964).
6. W. D. McGrath and J. J. McGarvey, Nature, 201, 991 (1964).
7. J. J. McGarvey and W. D. McGrath, Trans. Faraday Soc., 60, 2196 (1964).
8. I. M. Napier and R. G. W. Norrish, Nature, 208, 1090 (1965).
9. I. M. Napier and R. G. W. Norrish, Proc. Roy. Soc., 299A, 317 (1967).
10. G. E. McGraw and H. S. Johnston, Intern. J. Chem. Kinetics, 1, 89 (1969).
11. H. A. Wiebe, A. Villa, T. Hellman, and J. Heicklen, unpublished results, The Pennsylvania State University, (1970).
12. R. Renaud and L. C. Leitch, Canad. J. Chem., 32, 545 (1954).
13. J. G. Calvert and J. N. Pitts, Jr., "Photochemistry", John Wiley and Sons (1966), p. 463.
14. L. Phillips, J. Chem. Soc., 1961, 3082.
15. J. C. Calvert, private communication (1969).
16. J. Heicklen and N. Cohen, Adv. Photochem., 5, 157 (1968).
17. E. W. R. Steacie and G. T. Shaw, Proc. Roy. Soc., A146, 388 (1934).
18. G. R. McMillan, J. Phys. Chem., 67, 931 (1963).
19. B. E. Ludwig and G. R. McMillan, J. Am. Chem. Soc., 91, 1085 (1969).
20. D. L. Snyder, J. Kumari, and G. R. McMillan, General Motors Symposium, "Chemical Reactions in Urban Atmospheres," Warren, Michigan (1969).
21. E. A. Arden, L. Phillips, and R. Shaw, J. Chem. Soc., 1964, 5126.
22. J. Heicklen, Adv. Chem., No. 76, "Oxidation of Organic Compounds - II," 23 (1968).
23. I. M. Napier and R. G. W. Norrish, Proc. Roy. Soc., 299A, 337 (1967).

Table I: Effect of Irradiation Time on
the Photolysis of Mixtures of
 CH_3ONO and NO .

Irradiation Time, min	[NO], Torr	$\Phi \{\text{N}_2\text{O}\}$
Temp = 25°C, $[\text{CH}_3\text{ONO}] = 30 \text{ Torr}$, $I_a = 1.88 \times 10^{-6} \text{ Einstein/l-min}$		
5.00	1.83	0.088
30.00	1.04	0.093
30.00	1.49	0.086
30.00	2.18	0.085
50.00	3.18	0.087
100.00	0.82	0.084
200.00	1.18	0.084
Temp = 80°C, $[\text{CH}_3\text{ONO}] = 30 \text{ Torr}$, $I_a = 2.07 \times 10^{-6} \text{ Einstein/l-min}$		
50.00	1.29	0.072
100.00	1.42	0.075
100.00	1.51	0.072
120.00	1.38	0.074
200.00	1.30	0.066
Temp = 150°C, $[\text{CH}_3\text{ONO}] = \text{Torr}$, $I_a = 2.26 \times 10^{-6} \text{ Einstein/l-min}$		
63.00	0.72	0.075
120.00	1.33	0.073

Table II: Photolysis of Mixtures of CH_3ONO and NO at 25°C .

$[\text{CH}_3\text{ONO}]$, Torr	$[\text{NO}]$, Torr	Irradiation Time, min	$10^6 I_a$ Einstein/l-min	$\Phi\{\text{N}_2\text{O}\}$	$\Phi\{\text{N}_2\}$	$2\Phi\{\text{N}_2\text{O}\} + \Phi\{\text{N}_2\}$
2.30	1.09	20.00	0.38	0.25	Tr(a)	0.50
3.18	0.92	40.00	0.58	0.23	Tr	0.46
5.85	1.78	40.00	0.60	0.188	Tr	0.376
9.0	1.50	20.00	1.13	0.151	Tr	0.302
9.2	1.52	45.00	1.18	0.154	Tr	0.308
18	1.18	60.00	1.50	0.094	Tr	0.188
30	4.5	30.00	2.97	0.082	0.0049	0.169
30	8.8	30.00	2.97	0.078	0.0142	0.168
30	11	65.00	1.88	0.072	-	0.144
30	18	30.00	1.88	0.062	0.045	0.169
30	31	60.00	1.88	-	0.057	-
30	34	35.00	1.88	0.036	0.067	0.139
30	39	30.00	1.88	0.044	-	-
30	56	30.00	1.88	0.041	0.076	0.157
30	59	30.00	1.88	-	0.091	-
30	88	30.00	1.88	0.027	0.119	0.173
87	1.40	30.00	2.19	0.054	Tr	0.108
174	1.29	30.00	2.19	0.054	Tr	0.108
234	1.42	30.00	2.19	0.066	Tr	0.132

(a) Trace

Table III: Photolysis of Mixtures of CH_3ONO
and NO in the Presence of N_2 .
Irradiation Time = 30 Min.

$[\text{N}_2]$, Torr	$[\text{NO}]$, Torr	$\Phi\{\text{N}_2\text{O}\}$
Temp = 25°C , $[\text{CH}_3\text{ONO}] = 30$ Torr, $I_a = 1.88 \times 10^{-6}$ Einstein/l-min		
37	1.08	0.087
67	1.89	0.082
100	1.29	0.080
139	1.65	0.073
311	0.98	0.061
454	1.81	0.063
677	1.58	0.061

Temp = 80°C , $[\text{CH}_3\text{ONO}] = 30$ Torr, $I_a = 2.64 \times 10^{-6}$ Einstein/l-min		
0	0.94	0.078 ^(a)
79	0.87	0.068
144	1.30	0.061
213	1.55	0.059
314	1.42	0.052
571	1.00	0.051

Temp = 150°C , $[\text{CH}_3\text{ONO}] = 30$ Torr, $I_a = 2.23 \times 10^{-6}$ Einstein/l-min		
0	1.18	0.087
291	1.10	0.065
473	1.10	0.059
608	1.31	0.055

(a) Irradiation Time = 60 Min.

Table IV: Photolysis of Mixtures of CH_3ONO
and NO in the Presence of CO .

$[\text{CO}]/[\text{NO}]$	$[\text{NO}]$, Torr	$[\text{CO}]$, Torr	Irradiation Time, min	$\Phi\{\text{N}_2\text{O}\}$	$10^3 \Phi\{\text{CO}_2\}$
Temp = 25°C , $[\text{CH}_3\text{ONO}] = 20$ Torr, $I_a = 0.79 \times 10^{-6}$ Einstein/l-min					
4170	0.091	380	200.0	0.067	4.6
3670	0.089	327	360.0	0.066	4.0
2600	0.105	273	240.0	0.070	3.8
2490	0.095	235	270.0	0.063	3.7
905	0.093	84	300.0	0.084	2.8
903	0.112	101	272.0	0.084	2.8
876	0.105	92	125.0	0.079	2.7
703	0.108	76	184.0	0.084	2.9
Temp = 80°C , $[\text{CH}_3\text{ONO}] = 30$ Torr, $I_a = 2.16 \times 10^{-6}$ Einstein/l-min					
743	1.00	743	175.0	0.038	2.46
585	1.09	637	265.0	0.037	2.02
483	1.02	490	120.0	0.044	2.32
400	0.84	336	225.0	0.042	1.81
254	0.96	244	180.0	0.049	1.68
208	2.55	531	255.0	0.048	1.45
162	1.76	286	195.0	0.049	1.48
142	2.93	416	235.0	0.043	1.63
141	3.23	456	270.0	0.046	1.19
49	7.83	381	300.0	0.051	1.37
Temp = 150°C , $[\text{CH}_3\text{ONO}] = 30$ Torr, $I_a = 2.26 \times 10^{-6}$ Einstein/l-min					
1380	0.57	783	120.0	0.034	20.6
516	0.74	384	120.0	0.040	9.5
427	1.04	444	205.0	0.039	8.1
278	1.20	333	185.0	0.041	6.0
233	1.23	286	60.0	0.056	5.2
190	1.30	247	60.0	0.049	2.6
92	7.23	664	120.0	0.037	2.5

Table V: Photolysis of CH_3ONO

Temp., °C	$[\text{CH}_3\text{ONO}]$, Torr	$10^{17} I_a$, Einstein/l-min	$\Phi_f\{\text{N}_2\text{O}\}$	$\Phi_f\{\text{N}_2\}$	$\Phi_f\{\text{CO}\}$	$\Phi_f\{\text{NO}\}$
25	22	49	0.072	0.0014	0.0053	0.041
80	25	50	0.072	0.0014	0.0088	0.064
125	30	50	0.072	0.0014	0.0118	0.084

Table VI: Summary of Rate Constant Ratios

Ratio	Value	Units	Temp., °C	Source
$k_{5a}k_{5b}/k_{5a}k_{4a}^{1/2}$	62	$\underline{M}^{-3/2} \text{ sec}^{-1/2}$	25	Eqn. II, Fig. 5
$k_{5a}^{1/2}/k_{4a}$	0.020	$\underline{M}^{-1/2} \text{ sec}^{-1/2}$	25	Eqn. II, Fig. 5
k_{2a}/k_2	0.145	none	25	Eqn. III, Fig. 6
k_{2a}/k_2	0.145	none	all	Table III, Fig. 1
k_6/k_1	1.94	Torr	25	Eqn. III, Fig. 6
k_8/k_2	$\sim 5 \times 10^{-4}$	none	all	Table IV
k_{4a}/k_{4b}	51	none	all	$\Phi_f\{\text{N}_2\text{O}\}/\Phi_f\{\text{N}_2\}$

List of Figures

- Fig. 1 Plot of N_2O production vs. irradiation time in the photolysis of pure CH_3ONO at 25, 80, and 125°C .
- Fig. 2 Plot of N_2 production vs. irradiation time in the photolysis of pure CH_3ONO at 25, 80, and 125°C .
- Fig. 3 Plot of CO production vs. irradiation time in the photolysis of pure CH_3ONO at 25, 80, and 125°C .
- Fig. 4 Plot of NO production vs. irradiation time in the photolysis of pure CH_3ONO at 25, 80, and 125°C .
- Fig. 5 Log-log plot of $I_a^{1/2} \Phi\{\text{N}_2\}/(\Phi\{\text{N}_2\text{O}\})^{1/2}$ vs. $[\text{NO}]$ in the photolysis of $\text{CH}_3\text{ONO-NO}$ mixtures at 25°C and $[\text{CH}_3\text{ONO}] = 30 \text{ Torr}$.
- Fig. 6 Plot of $2 \Phi\{\text{N}_2\text{O}\} + \Phi\{\text{N}_2\}$ vs. $[\text{CH}_3\text{ONO}]^{-1}$ in the photolysis of $\text{CH}_3\text{ONO-NO}$ mixtures at 25°C .
- Fig. 7 Log-log plot of $\Phi\{\text{CO}_2\}/\Phi\{\text{N}_2\text{O}\}$ vs. $[\text{CO}]/[\text{NO}]$ in the photolysis of $\text{CH}_3\text{ONO-NO-CO}$ mixtures at 150°C .

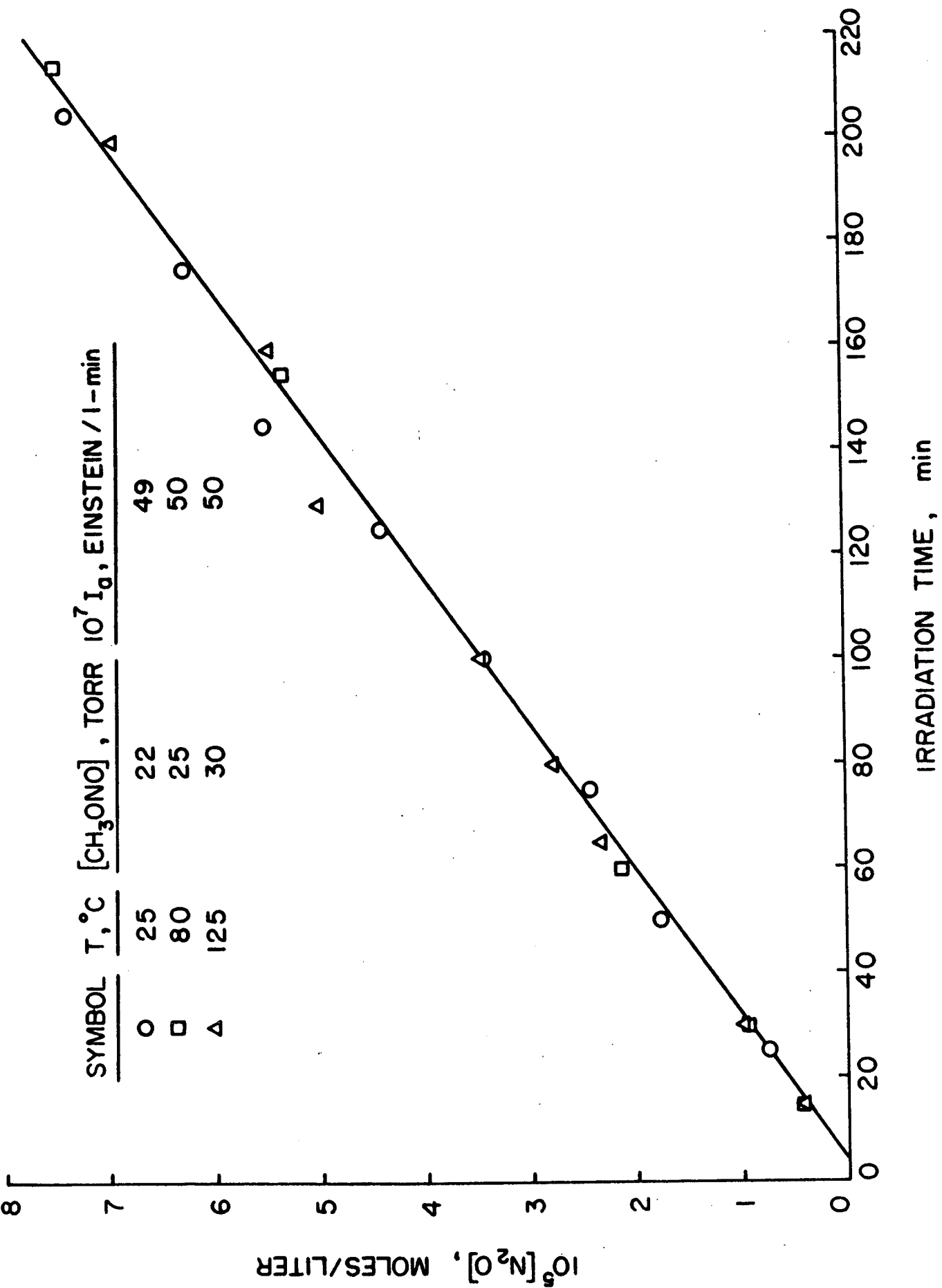


Figure 1

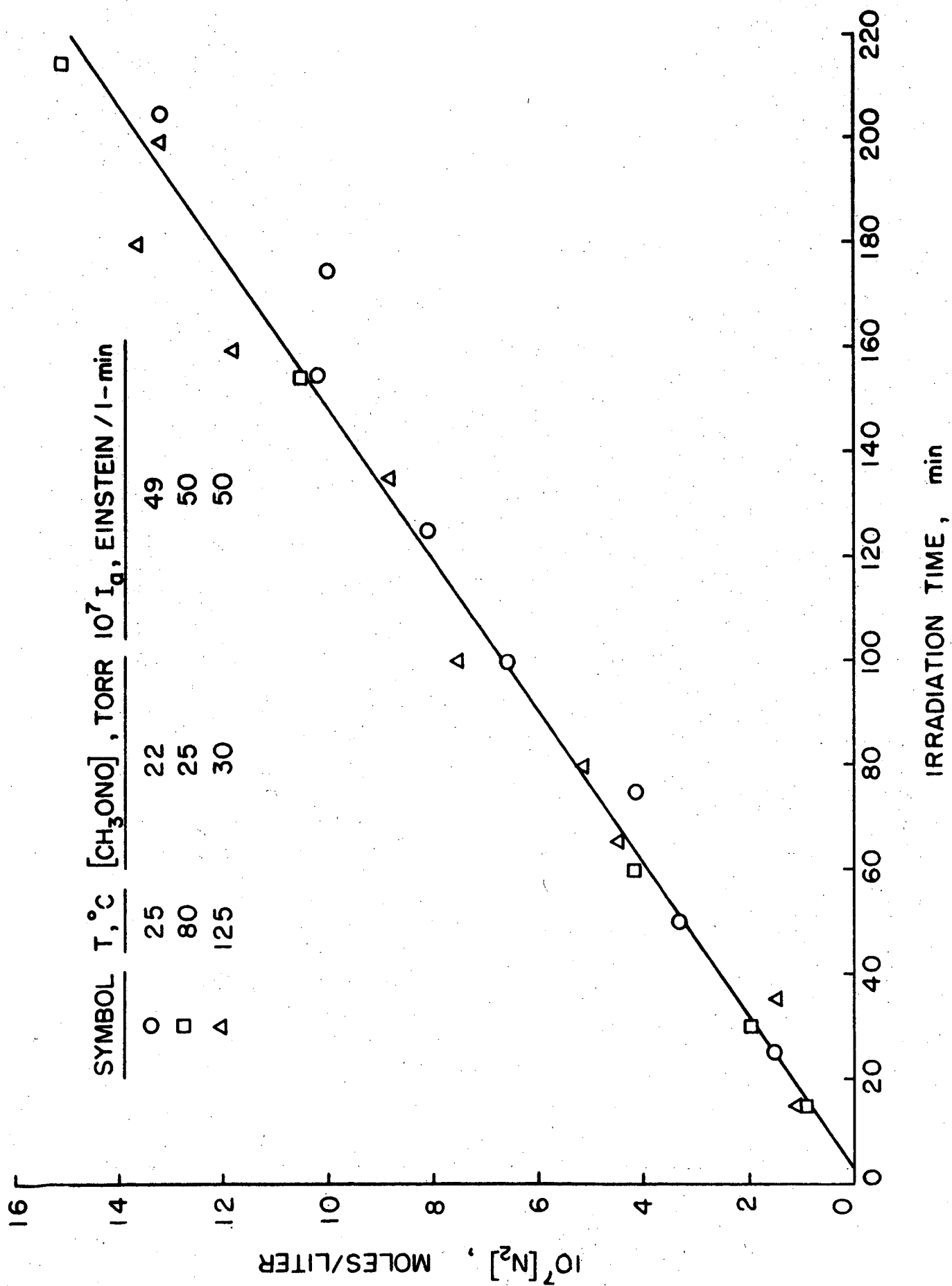


Figure 2

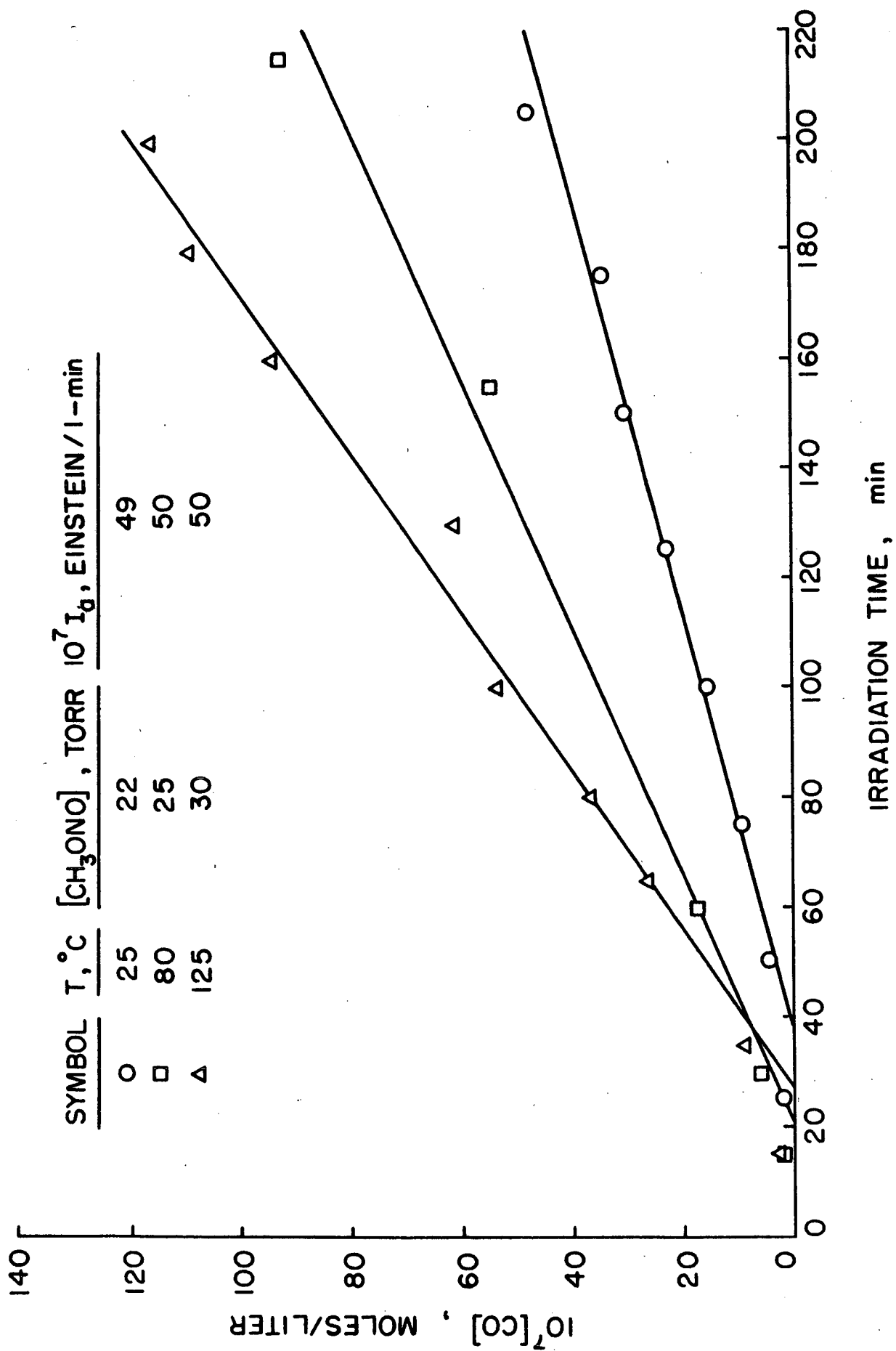
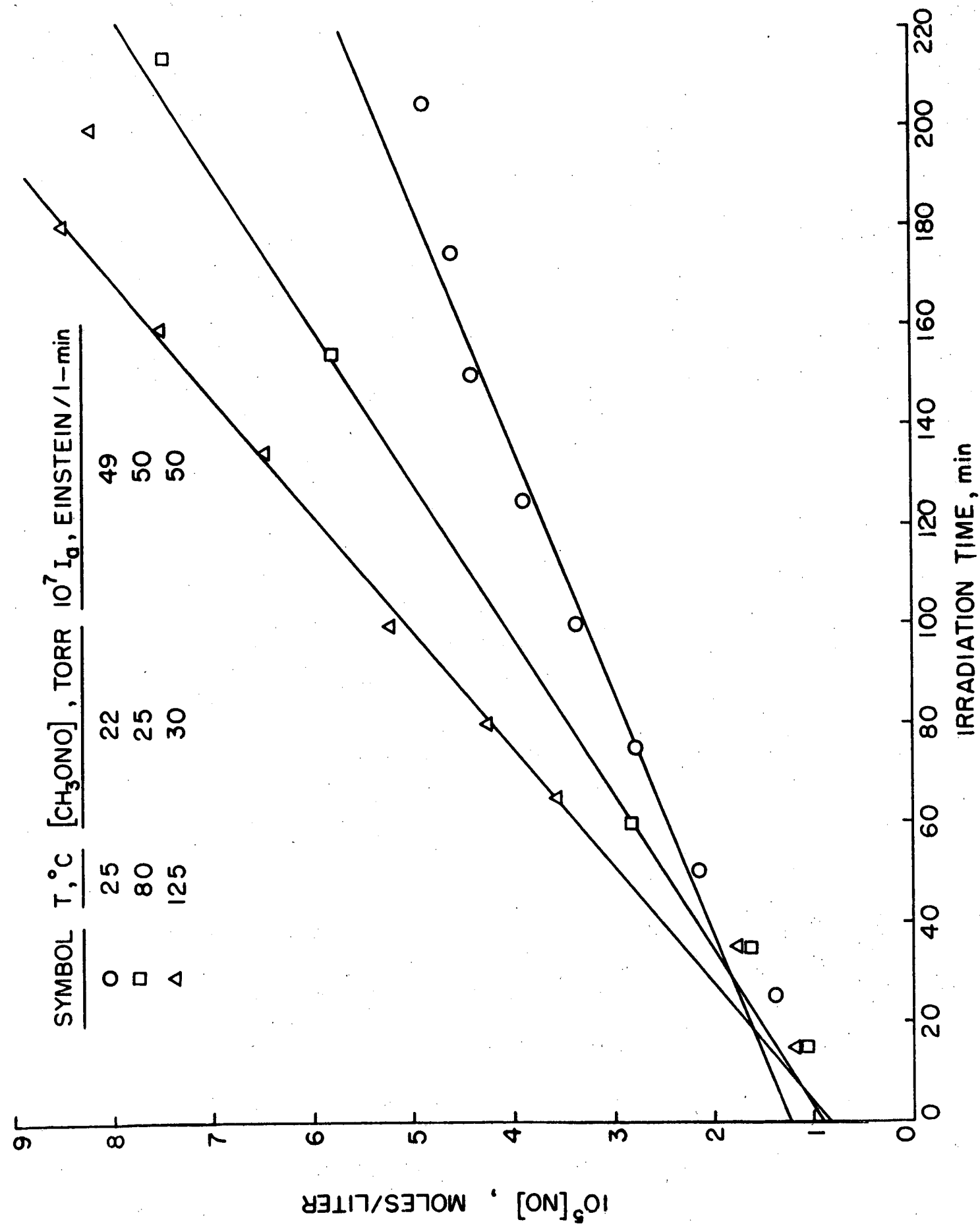


Figure 3



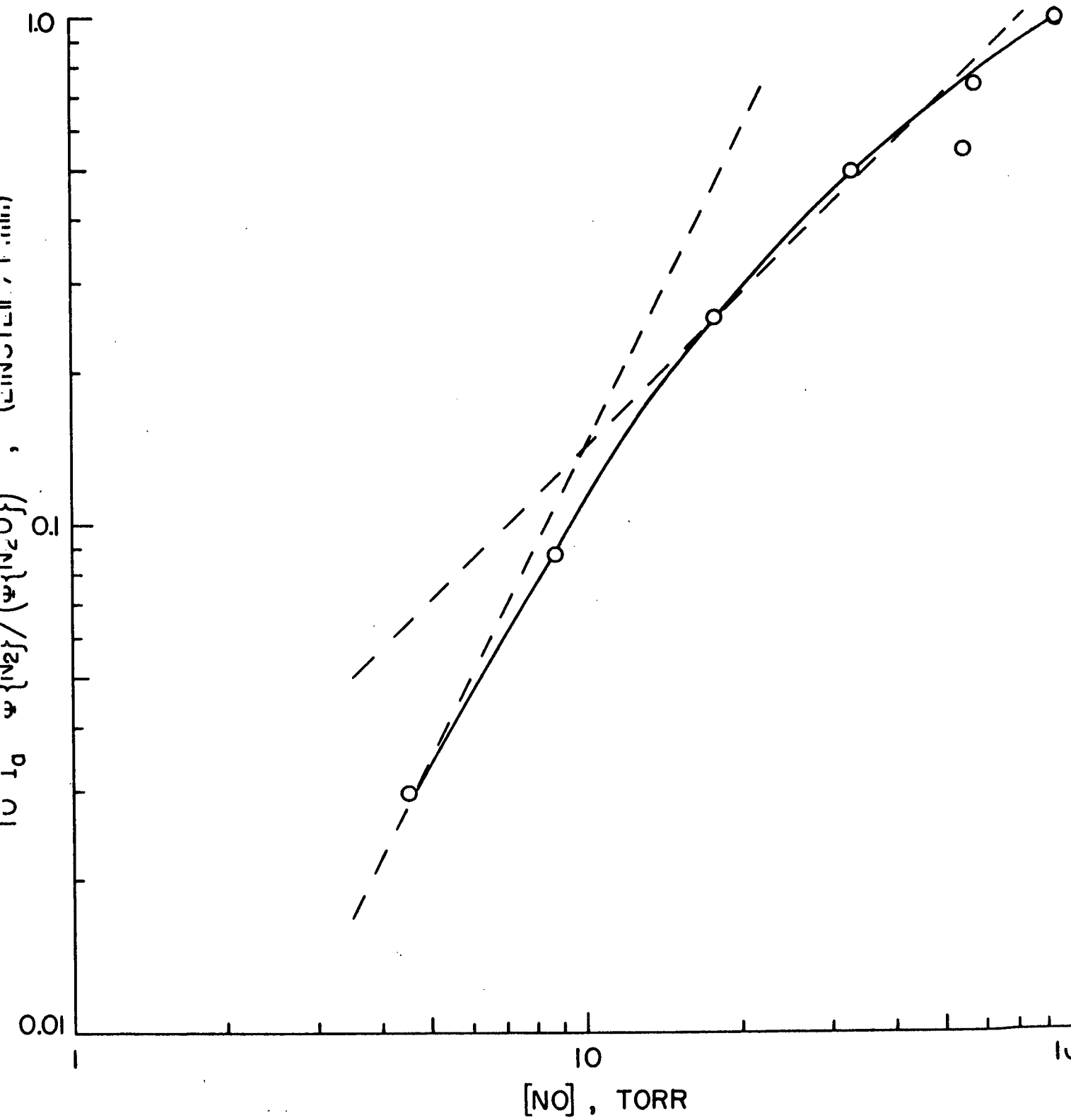


Figure 5

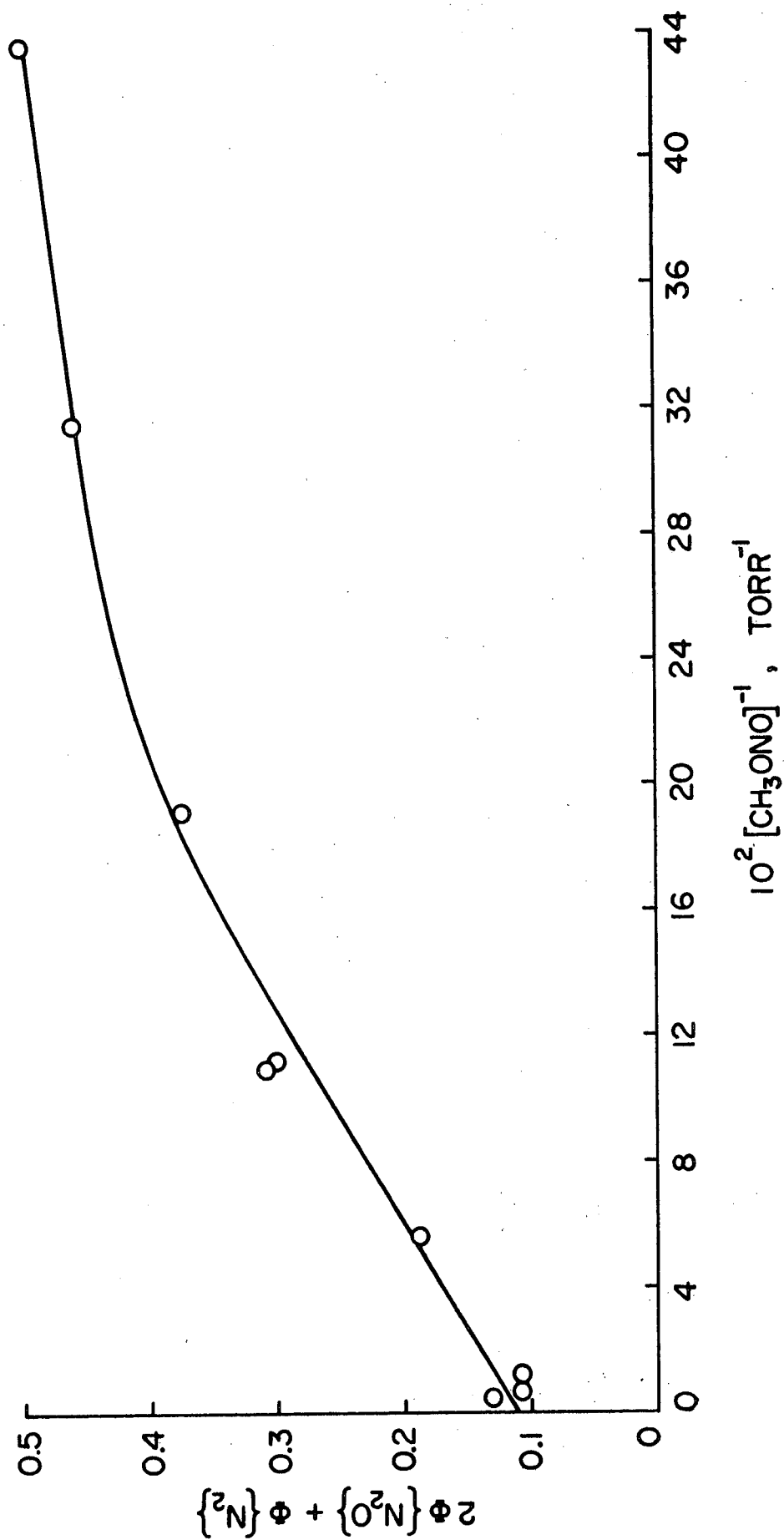


Figure 6

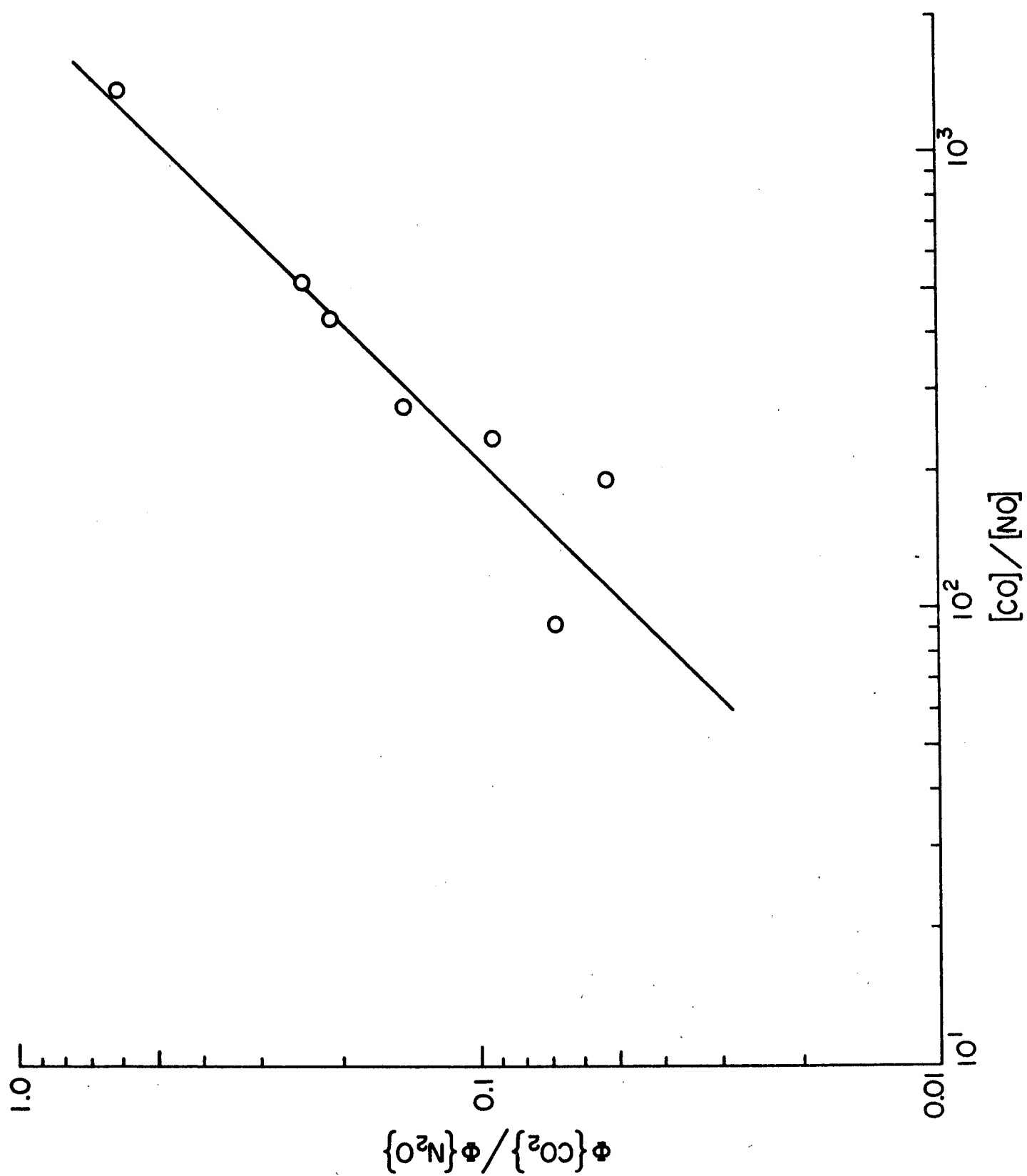


Figure 7